ORIGINAL RESEARCH ARTICLE

WILEY Journal of Cellular Physiology

MicroRNA-16 functions as a tumor-suppressor gene in oral squamous cell carcinoma by targeting AKT3 and BCL2L2

Xi Wang* | Guang-hui Li* 🔟

Department of Stomatology, The First Affiliated Hospital of Zhengzhou University, Zhengzhou, China

Correspondence
Guang-hui Li, Department of Stomatology, The First Affiliated Hospital of Zhengzhou University, No. 1 East Jian She Road, Zhengzhou 450052, China.
Email: franklin1082@163.com

Aberrant expressions of microRNAs have been reported to be strongly associated with the progression and prognosis of various tumors, including oral squamous cell carcinoma (OSCC). Recent studies on miRNA expression profiling have suggested that microRNA-16 (miR-16) may be dysregulated in OSCC. However, the tumorigenic roles and mechanisms of miR-16 in OSCC are still largely unknown. In this study, we demonstrated that miR-16 was specifically downregulated in both OSCC patients and cancer cell lines. In addition, functional roles of miR-16 in vitro suggested that the miR-16 mimic inhibited cell proliferation and induced apoptosis, whereas miR-16 inhibitor displayed the opposite effects. Luciferase reporter assay and correlation analysis showed that AKT3 and BCL2L2 were directly targeted by miR-16 and were inversely expressed with miR-16 in OSCC. Moreover, restoration of AKT3 and BCL2L2 expression could partially reverse the cell proliferation inhibition and apoptosis induction caused by miR-16. In xenograft nude mice, miR-16 mimics decreased the expression of AKT3 and BCL2L2 and reduced the tumors volumes and weights, whereas the miR-16 inhibitor exhibited adverse effects in the derived xenografts. In conclusion, the findings suggested that miR-16 functions as a tumor suppressor miRNA to inhibit cell proliferation and induce apoptosis in OSCC through decreasing the oncogenes AKT3 and BCL2L2 and that miR-16 could be a potential therapeutic target for OSCC.

KEYWORDS
AKT3, BCL2L2, microRNA-16 (miR-16), oral squamous cell carcinoma (OSCC)

1 | INTRODUCTION

Oral squamous cell carcinoma (OSCC) is the most common head and neck cancer and the predominant histological type of oral cavity cancer (Chi, Day, & Neville, 2015). It broadly encompasses malignancies in the lips, tongue, pharynx, hard palate, and alveolar ridges with a high mortality rate and a poor prognosis. Elderly patients between 45 and 75 years of age are susceptible to developing OSCC (Omar, 2015). The

major risk factors for the development of OSCC include both intrinsic and extrinsic factors, including tobacco intake, alcohol drinking, HPV infection, and poor diet (Rivera, Oliveira, Costa, De Rossi, & Paes Leme, 2017). Despite considerable advances in curative multimodal treatments, the overall survival rate in patients with OSCC has not markedly improved (Fukumoto et al., 2015). Therefore, there is an urgent need to gain a thorough understanding of molecular oncogenic mechanisms underlying OSCC and to uncover novel diagnostic biomarkers or therapeutic targets.

MicroRNAs (miRNAs) are endogenous single-stranded noncoding RNAs approximately 22 nucleotides in length (Osada & Takahashi, 2007). It regulates protein-coding gene expression by binding to the

Abbreviations: HIOEC, human immortalized oral epithelial cells; miRNA, microRNA; Mut, mutation; NC, negative control; OSCC, oral squamous cell carcinoma; UTR, untranslated region; Wt, wild type.

*Wang and Li have contributed equally to this study.

- -

complementary sequences in the 3′-untranslated region (UTR) of target mRNAs (Lin & Gregory, 2015). More than 2,500 human miRNAs have been reported to date and over 30% of the human genes are predicted to be regulated by these miRNAs. Increasing evidence suggests that miRNAs are aberrantly expressed in multiple human tumors and involved in critical oncogenesis processes such as cell proliferation, differentiation, migration, and invasion (Lai et al., 2018). Dysregulation of miRNAs has been reported to be strongly associated with the progression and prognosis of OSCC (Tu, Lin, & Chang, 2013). In particular, a number of miRNAs, for example, miR-22, miR-124, miR-433, and miR-375 (Feng, Luo, Wang, Zhang, & Chen, 2018; Hunt, Jones, Hinsley, Whawell, & Lambert, 2011; Wang et al., 2017; Zhang et al., 2017), have been reported to inhibit OSCC cell growth, migration, and apoptosis, and have been recognized as novel targets in OSCC diagnosis and therapy.

In a recent study, microRNA-16 (miR-16) was identified to be downregulated in OSCC tissues (Manikandan et al., 2016). miR-16 is a novel cancer-associated miRNA and has been recognized as a tumor suppressor in different types of human cancers, including breast cancer (Guo, Connick, Vanderhoof, Ishak, & Hartley, 2015), colorectal cancer (Ma et al., 2013), bladder cancer (Jiang, Liu, & Yuan, 2013), gastric adenocarcinoma (Kang et al., 2015), and hepatocellular carcinoma (Wu, Wang, Yao, & Li, 2015). However, the role of miR-16 in OSCC and the underlying molecular mechanism remain to be delineated.

In the current study, we aimed to investigate the expression level of miR-16 in OSCC tissues and cell lines and assess the effect of miR-16 on cell proliferation and apoptosis. Moreover, the mechanisms underlying the role of miR-16 together with its target genes in OSCC progression were also explored in OSCC cells and animal models.

2 | MATERIALS AND METHODS

2.1 | Ethics statement

This study was approved by the Ethical Review Committee of Zhengzhou University. Informed consent was obtained from all participants and/or their legal guardians. Animal experiments were conducted following the National Institutes of Health Guidelines for the Use of Laboratory Animals.

2.2 | Patients and samples

OSCC samples and adjacent normal tissues were collected from 18 patients who underwent surgical treatment in the Department of Stomatology, The First Affiliated Hospital of Zhengzhou University, between September 2015 and June 2017. Patients who had received chemotherapy, radiotherapy, or related treatment before surgery were excluded. The tissue samples were immediately frozen in liquid nitrogen after operation and stored at −80°C for RNA extraction.

2.3 | Cell culture and transfection

Human immortalized oral epithelial cells (HIOEC) and five human OSCC cell lines (SCC-4, SCC-25, HN-6, CAL-27, and TCA-83) were purchased

from the Type Culture Collection of the Chinese Academy of Science (Shanghai, China). Cells were maintained in Dulbecco modified Eagle's medium (Gibco, Invitrogen Corporation, Carlsbad, CA) with 10% fetal bovine serum (Gibco) and 1% penicillin/streptomycin at 37°C in a standard humidified incubator containing 5% CO_2.

The miR-16 mimic, the miR-16 inhibitor, and their corresponding negative control (miR-16 mimic NC and miR-16 inhibitor NC) were purchased from RiboBio Co., Ltd. (Guangzhou, China). SCC-25 and CAL-27 cells were transfected with the above mimic/inhibitor or corresponding negative control for 48 hr using Lipofectamine 2000 (Life Technologies, Waltham, MA) according to the manufacturer's protocol. For the overexpression of AKT3 and BCL2L2, the cDNA of AKT3 or BCL2L2 was cloned into the mammalian expression vector pcDNA3.1 (Invitrogen, Waltham, MA), respectively, to construct two overexpressed vectors; pcDNA3.1-AKT3 and pcDNA3.1-BCL2L2. The pcDNA3.1 was used as a NC.

2.4 | Cell proliferation and apoptosis assay

Cell proliferation was detected using a Cell Counting kit-8 (CCK-8; Beyotime, Shanghai, China) assay. Transfected cells were seeded in 96-well plates at 5×10^3 cells/well, and cultured for 0, 24, 48, 72, 96, or 120 hr. Ten microliter of CCK-8 reagent was added to each well and cells were then incubated for 1.5 hr at 37°C. The absorbance was determined at a wavelength of 450 nm with a microplate reader. Data were collected from triplicate experiments. For the apoptosis assay, transfected cells were stained with FITC-conjugated Annexin V and PI using an Annexin V-FITC Apoptosis Detection Kit (Beyotime) according to the manufacturer's instructions. The cell apoptosis was detected using the Attune NxT Flow Cytometer (Thermo Scientific, MA).

2.5 | Luciferase reporter assay

Target genes of miR-16 were predicted with TargetScan 7.1 (http://www.targetscan.org/). The dual luciferase reporter vectors carrying wild-type (Wt) AKT3 3′-UTR and BCL2L2 3′-UTR as well as the corresponding mutation (Mut) 3′-UTR with deletion of the miR-16-binding site were constructed (Ribio Co., Guangzhou, China). SCC-25 cells were cotransfected with the AKT3/BCL2L2 3′-UTR Wt or Mut plasmid along with the miR-16 mimic or the NC. After 48 hr of transfection, cells were collected and luciferase activities were analyzed using a dual luciferase reporter assay kit (Promega, Madison, WI) according to the manufacturer's instructions. All experiments were performed at least three times.

2.6 | Western blot analysis

Total proteins of cells and tumors were isolated with RIPA buffer (Beyotime) and the proteins concentrations were determined using a Pierce Bicinchoninic acid Protein Assay Kit (Beyotime). Proteins were separated by SDS-PAGE (about 8%–10%) and then transferred to polyvinylidene fluoride membranes. The membrane was blocked with 5% nonfat milk at room temperature for 1 hr and incubated at 4°C overnight

with the primary antibodies: anti-AKT3 (1:1,000; Abcam, Cambridge, UK) and anti-BCL2L2 (1:1,000; CST, Boston, MA). The membranes were subsequently incubated with the appropriate secondary antibodies at room temperature for 1 hr. Bands were visualized using the standard enhanced chemiluminescence procedure. β-Actin was used as a loading control. Quantitative analysis was performed by measurement of the gray-scale value of the bands using Image J software (National Institutes of Health, Bethesda, MD). Data were obtained from three independent experiments.

2.7 | Quantitative reverse transcription polymerase chain reaction

Total RNA from tissues and cells was isolated using TRIzol reagent (Invitrogen) according to the manufacturer's protocol. Reverse transcription of miRNA and mRNA was performed using the TaqMan MicroRNA Reverse Transcription Kit and the M-MLV 1st Strand Kit (Invitrogen), respectively. PCR amplification was performed in triplicate for 10 min at 95℃, followed by 40 cycles of 95℃ for 15 s and an annealing step at 60℃ for 40 s using an ABI PRISM 7500 Sequence Detection System (Thermo Scientific, MA). Fold change was calculated using the $2^{-\Delta\Delta Ct}$ method. The CT values of U6 and glyceraldehyde-3-phosphate dehydrogenase (GAPDH) were used as the internal controls to normalize the relative expression levels of miR-16 and its target genes, respectively. The primers used are as follows: miR-16, 5′-TAGCAGCACGTAAATA TTGGCG-3′; U6, 5′-CGCAAGGATGACACGCAAATTC-3′; AKT3, forward 5′-TTGCTTTCAGGGCTCTTGAT-3′ and reverse 5′-CATAATTTCTTTTG CATCATCTGG-3′; BCL2L2, forward 5′-AGGGTTATGTCTGTGGAGCTG -3′ and reverse 5′-AGCGGGTCTCGAACTCATC-3′; GAPDH, forward 5′-GCACAAGAGGAAGAGAGAGACC-3′ and reverse 5′-AGGGGAGATT CAGTGTGGTG-3′.

2.8 | Animal experiments

A total of forty 6-week-old male BALB/c nude mice (20–25 g) were purchased from Beijing HFK Bioscience Co., Ltd (Beijing, China) and were fed in the specific pathogen-free laboratory at room temperature (22–25 °C) with appropriate relative humidity (50%–60%), as well as sterile padding, food, and water. Mice were divided into five groups (eight mice per group): the control, miR-16 mimic NC, miR-16 mimic, miR-16 inhibitor NC, and miR-16 inhibitor. Equal numbers of 2×10^6 SCC-25 cells transfected with the miR-16 mimic/inhibitor or scramble were injected subcutaneously into the dorsal region of each mouse. Tumor size was measured every three days and calculated as length × width^2/2. Mice were killed on the 27th day after inoculation, and the tumor was then surgically removed and weighed. Tumor tissues were immediately placed in liquid nitrogen for RNA and protein extraction.

2.9 | Statistical analysis

All data were presented as means ± standard deviation and analyzed with Prism 6 (GraphPad Software, CA). Student t test was used to determine the significance between two independent groups. One-way analysis of variance, followed by Dunnett's test were used to conduct the multiple comparisons. Pearson correlation analysis was used to determine the correlations between miR-16 and AKT3 or BCL2L2 expression. $p < 0.05$ was considered statistically significant.

3 | RESULTS

3.1 | miR-16 is downregulated in OSCC tissues and cell lines

The expression levels of miR-16 were investigated by quantitative reverse transcription polymerase chain reaction (qRT-PCR) in OSCC and adjacent nontumorous tissues. Results showed that miR-16 expression was significantly decreased in OSCC tissues compared with adjacent normal tissues ($p < 0.05$; Figure 1a). This result was confirmed in human OSCC cell lines (SCC-4, SCC-25,
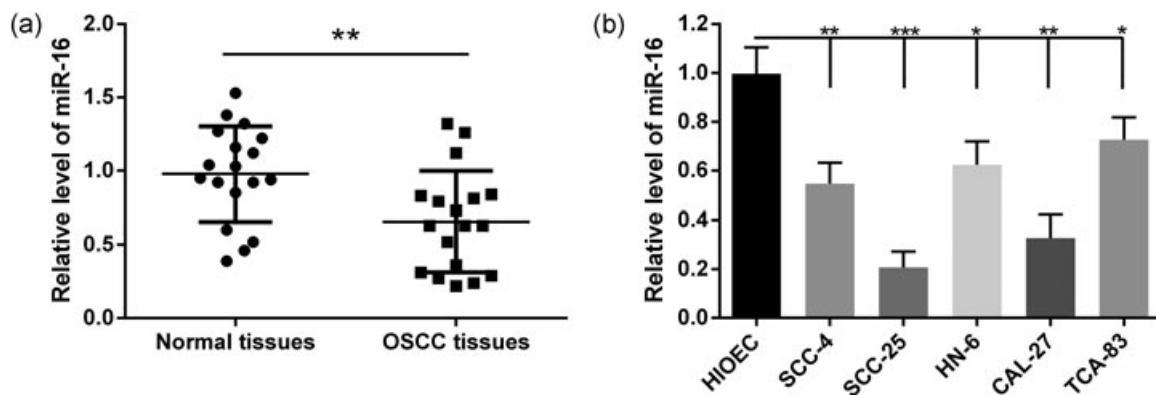

FIGURE 1 miR-16 is downregulated in oral squamous cell carcinoma (OSCC) tissues and cell lines. (a) The relative expressions of miR-16 in eighteen OSCC patients and their matched normal tissues were determined by qRT-PCR. (b) The relative expressions of miR-16 in five OSCC cell lines and a human immortalized oral epithelial cells (HIOEC) were checked by qRT-PCR. Data were presented as mean ± standard deviation for three independent experiments. *$p < 0.05$, **$p < 0.01$, ***$p < 0.001$ versus normal tissues or HIOEC cells. miR-16, microRNA-16; qRT-PCR, quantitative reverse transcription polymerase chain reaction

HN-6, CAL-27, TCA-83); compared with HIOEC normal cells, miR-16 showed low expression in the five OSCC cell lines than HIOEC (Figure 1b). Besides, the down expression of miR-16 was more noticeable in SCC-25 and CAL-27 cells. Thus, these two cell lines were used in further studies.

3.2 | miR-16 inhibits proliferation and induces apoptosis in OSCC cells

The significant decrease in miR-16 expression in OSCC samples and cell lines prompted us to explore the possible biological function of miR-16. The miR-16 mimic/inhibitor and the corresponding NC were transfected into SCC-25 and CAL-27 cell lines, respectively. qRT-PCR was performed to monitor transfection efficiency at 48 hr after transfection. As shown in Figure 2a,c, the miR-16 mimic significantly increased miR-16 expression, whereas the inhibitor decreased the expression of miR-16 ($p < 0.05$). To explore whether miR-16 could influence the proliferation of OSCC cells, the CCK-8 assay was carried out to assess cell viability. Compared with the NC group, the miR-16 mimic suppressed the cell viability of SCC-25 and CAL-27 cells. Additionally, it was found

that the miR-16 inhibitor significantly promoted cell viability (Figure 2b,d). Furthermore, an Annexin V/PI staining analysis was performed to investigate the function of miR-16 in cell apoptosis. We found that the apoptotic rate was significantly increased in miR-16 mimic transfected cells; conversely, the apoptotic rate was decreased after the expression of miR-16 was inhibited in SCC-25 and CAL-27 cells (Figure 3). All these results indicated that miR-16 could reduce proliferation and induce apoptosis in OSCC cells.

3.3 | miR-16 directly targets the 3′-UTR of AKT3 and BCL2L2

To elucidate the molecular mechanisms by which miR-16 exerts its functional effects on OSCC cells, TargetScan 7.1, an online miRNA target algorithm, was used to predict the potential downstream targets of miR-16. Among the miR-16 targets, the 3′-UTR of AKT3 and BCL2L2 contain a site complementary to the seed region of miR-16 (Figure 4a,b). To determine whether AKT3 and BCL2L2 are direct targets of miR-16, the Wt sequence of AKT3 or BCL2L2 3′-UTR as well as the Mut sequence of AKT3 or BCL2L2 3′-UTR without the miR-16 target site
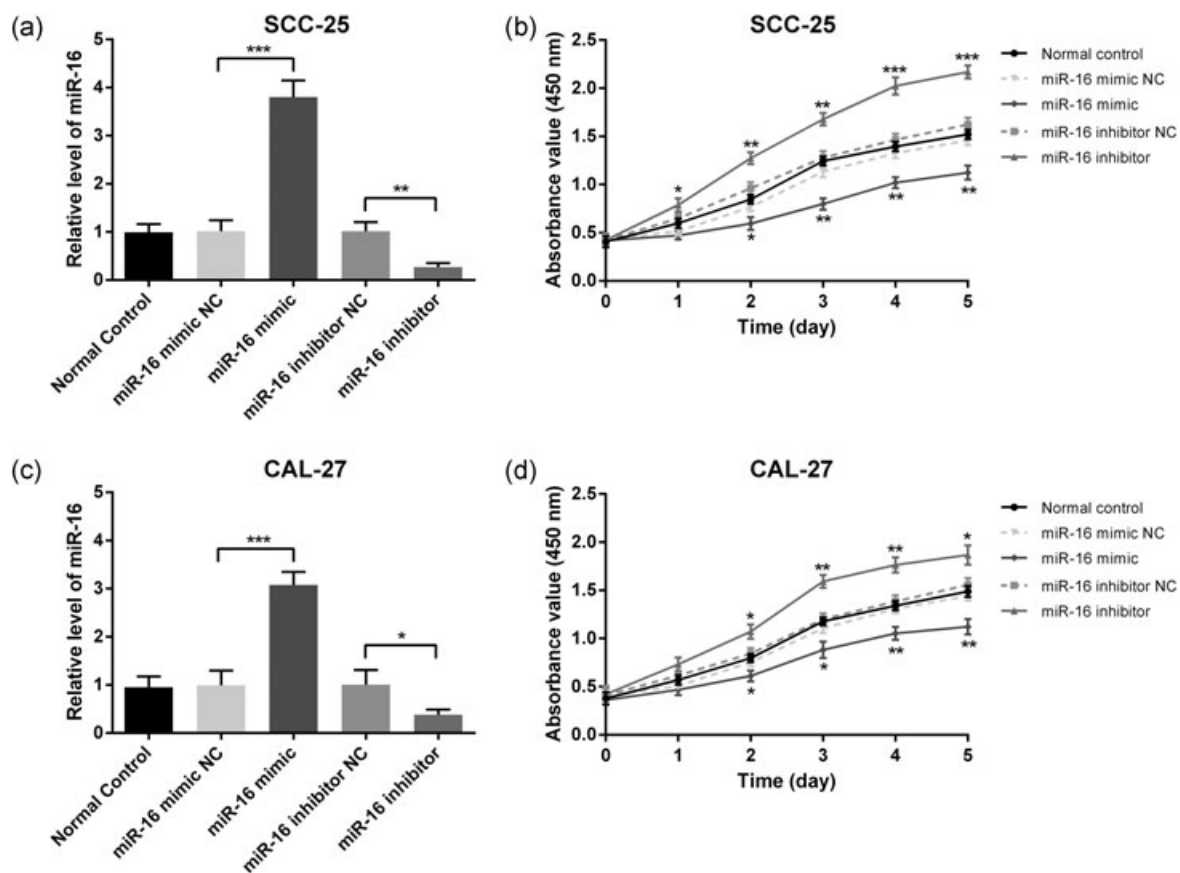

FIGURE 2 miR-16 inhibits the proliferation of SCC-25 and CAL-27 cell lines. The miR-16 mimic/inhibitor and the corresponding negative control were transfected into SCC-25 and CAL-27 cell lines, respectively. The relative expressions of miR-16 in SCC-25 (a) and CAL-27 (c) cells were determined at 48 hr after transfection by qRT-PCR. Cell proliferation of SCC-25 (b) and CAL-27 (d) was measured at 24, 48, 72, 96, and 120 hr after transfection by the CCK-8 assay. Data were presented as mean ± standard deviation for three independent experiments. *$p < 0.05$, **$p < 0.01$, ***$p < 0.001$ versus negative control. miR-16, microRNA-16; qRT-PCR, quantitative reverse transcription polymerase chain reaction
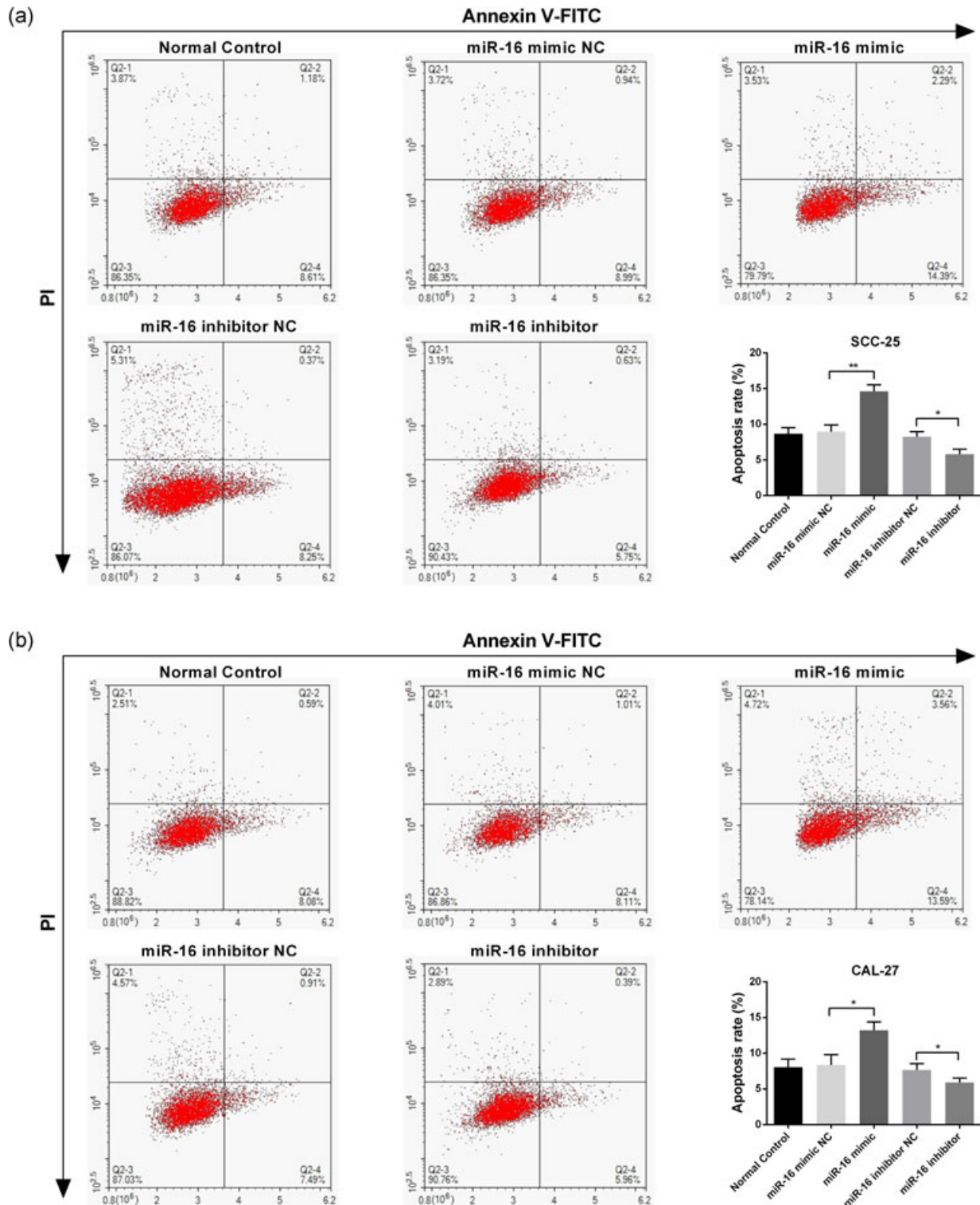
FIGURE 3 miR-16 induces apoptosis of SCC-25 and CAL-27 cell lines. The miR-16 mimic/inhibitor and the corresponding negative control were transfected into SCC-25 and CAL-27 cell lines, respectively. Annexin V/PI staining analysis was performed to investigate the apoptosis rate of SCC-25 (a) and CAL-27 (b) cells. Data were presented as mean ± standard deviation for three independent experiments. *$p < 0.05$, **$p < 0.01$, ***$p < 0.001$ versus negative control. miR-16, microRNA-16 [Color figure can be viewed at wileyonlinelibrary.com]

were inserted into the luciferase reporter vector. These vectors were then cotransfected into SCC-25 cells. The luciferase reporter assay revealed that the miR-16 mimic had no significant effect on the luciferase activity of either Mut-AKT3 or Mut-BCL2L2. In contrast, miR-16

overexpression significantly decreased the luciferase activity of Wt-AKT3 and Wt-BCL2L2 (Figure 4c,d). Collectively, the above data suggested that the AKT3 and BCL2L2 transcripts are genuine downstream targets of miR-16 in OSCC cells.
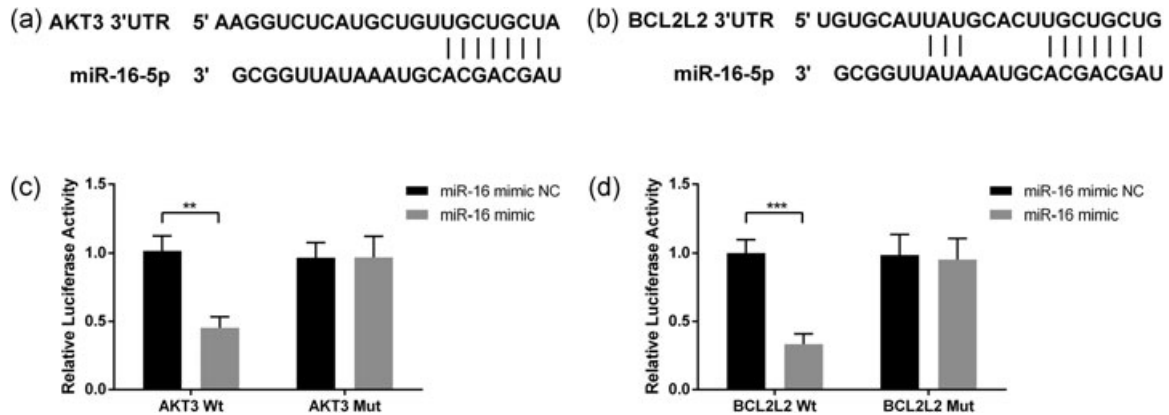
FIGURE 4 miR-16 directly targets the 3′-UTR of AKT3 and BCL2L2. TargetScan 7.1 was used to predict the potential downstream targets of miR-16. Sequence alignment between miR-16 and 3′-UTR of AKT3 (a) and BCL2L2 (b). Effects of miR-16 on 3′-UTR of AKT3 (c) or BCL2L2 (d) were determined by the Luciferase activity assay. Wild type and mutation AKT3 or BCL2L2 were inserted into the luciferase reporter vector and then cotransfected into SCC-25 cells with miR-16. After 48 hr of transfection, luciferase activities were measured. Data were presented as mean ± standard deviation for three independent experiments. **$p < 0.01$, ***$p < 0.001$ versus the negative control. miR-16, microRNA-16; UTR, untranslated region

3.4 | miR-16 negatively relates to AKT3 and BCL2L2

Pearson correlation analysis of miR-16 and AKT3 or BCL2L2 expression in the OSCC patient cohort suggested that miR-16 was negatively associated with AKT3 ($r = −0.62$, $p = 0.0057$) and BCL2L2 ($r = −0.68$, $p = 0.0017$; Figure 5a,b). To further confirm the inhibitory regulation of miR-16 on AKT3 and BCL2L2 expression, the mRNA levels of AKT3 and BCL2L2 were determined by qRT-PCR in miR-16 mimic- or inhibitor- transfected SCC-25 and CAL-27 cells. As shown in Figure 5c, the miR-16 mimic significantly reduced the mRNA level of AKT3, whiereas the miR-16 inhibitor played an opposing role in AKT3 expression. Similar interactions were also observed between miR-16 and BCL2L2 expression (Figure 5d).

3.5 | Overexpression of AKT3 and BCL2L2 promotes proliferation and inhibits apoptosis in OSCC cells

To further investigate whether the regulatory action of miR-16 on cell proliferation and apoptosis was mediated by its target genes AKT3 and BCL2L2, overexpression vectors of AKT3 and BCL2L2 were constructed and cotransfected with miR-16 into SCC-25 cells. Western blot analysis demonstrated that the protein expression of AKT3 downregulated by the miR-16 mimic was restored after pcDNA3.1-AKT3 transfection (Figure 6a). Furthermore, the restoration of AKT3 could partly overcome the inhibitory effects of miR-16 on cell proliferation (Figure 6b). Moreover, overexpression of AKT3 also significantly inhibited the apoptosis of SCC-25 cells induced by miR-16 (Figure 6c,d). Similarly, the expression of BCL2L2 was upregulated after pcDNA3.1-BCL2L2 transfection, which also partly reversed the regulatory action of miR-16 on cell proliferation and apoptosis (Figure 7).

3.6 | miR-16 inhibits SSC-25 engrafted tumor growth in vivo

To evaluate the effects of miR-16 on OSCC growth in vivo, SCC-25 cells transfected with the miR-16 mimic/inhibitor or scramble were injected into nude mice to generate an xenograft model. Tumors grew more slowly and had a markedly smaller size and lower weight in the miR-16 mimic-transfected group compared with the NC group, whereas tumors in the miR-16 inhibitor group grew faster (Figure 8a,b).

Meanwhile, expression levels of miR-16 and its target genes AKT3 and BCL2L2 in the derived xenografts were measured at 27 days after injection. The data indicated that miR-16 expression was stably regulated by the miR-16 mimic and inhibitor (Figure 8c). The protein expressions of AKT3 and BCL2L2 were decreased in the miR-16 mimic-transfected group and increased in the miR-16 inhibitor group (Figure 8d,e). Taken together, these results suggested that miR-16 functions as a tumor-suppressor miRNA in OSCC through decreasing the oncogenes AKT3 and BCL2L2 (Figure 9).

4 | DISCUSSION

In this study, we demonstrated that miR-16 was downregulated in OSCC tissues and cell lines. Overexpression of miR-16 significantly inhibited cell proliferation and induced apoptosis. Further studies identified AKT3 and BCL2L2, two critical oncogenes, as targets of miR-16. A significant negative regulation was found between miR-16 and AKT3 or BCL2L2 mRNA levels in both the OSCC patients and cell lines. Consistently, overexpression of AKT3 and BCL2L2 apparently promoted cell proliferation and inhibited apoptosis. In addition, in xenograft models, upregulation of miR-16 significantly inhibited tumor growth, whereas downregulation of miR-16 promoted progression of OSCC.

Accumulating researches have suggested that the aberrant expression of miRNAs is involved in the cancer pathogenicity,
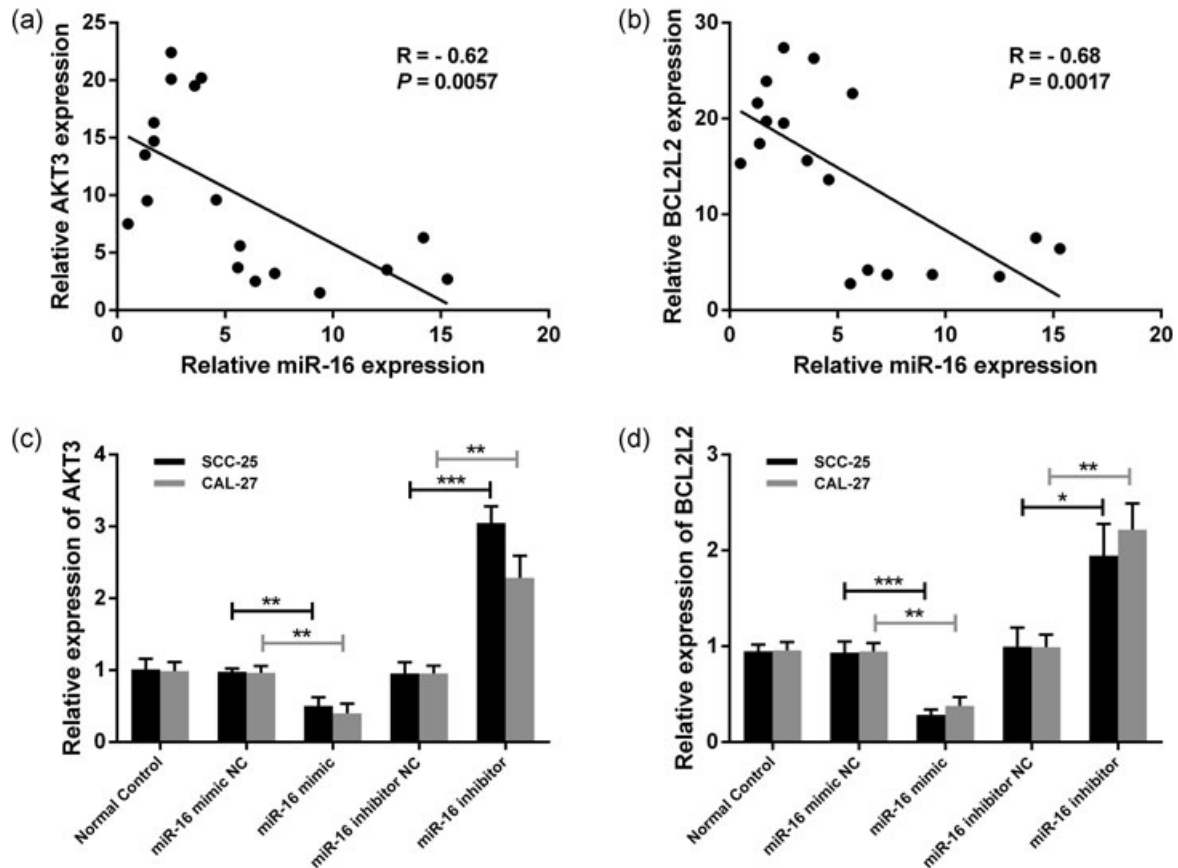
FIGURE 5 miR-16 negatively relates to AKT3 and BCL2L2. Pearson correlation analysis of miR-16 and AKT3 (a) or BCL2L2 (b) expression in the OSCC patient cohort. The relative expressions of AKT3 (c) or BCL2L2 (d) were detected by qRT-PCR in the miR-16 mimic/inhibitor or scramble-transfected SCC-25 and CAL-27 cells. Data were presented as mean ± standard deviation for three independent experiments. *$p < 0.05$, **$p < 0.01$, ***$p < 0.001$ versus the negative control. miR-16, microRNA-16; OSCC, oral squamous cell carcinoma; qRT-PCR, quantitative reverse transcription polymerase chain reaction

including OSCC, and miRNAs have been identified as potential prognostic biomarkers or therapeutic targets of OSCC (Radhika, Jeddy, Nithya, & Muthumeenakshi, 2016). A recent study of microarray profiling identified 46 differentially expressed miRNAs in OSCC (Manikandan et al., 2016). MiR-16, as one of the downregulated miRNA, aroused our great interest, since miR-16 was reported to have lower expression in multiple tumors as well. However, the tumorigenic roles and mechanisms of miR-16 in OSCC are still largely unknown. Here, we confirmed that miR-16 was significantly downregulated in OSCC tissues and cell lines. Meanwhile, compared with other cell lines, the expression of miR-16 is the lowest in SCC-25 and CAL-27. Thus, these two cell lines were chosen for further studies.

Cell proliferation and apoptosis are two crucial hallmarks of tumors and are factors directly correlated with cancer development. Previous studies showed that overexpression of miR-16 declined cellular proliferation and induced apoptosis in hepatocellular carcinoma and breast cancer cells (Mobarra et al., 2015; Wu et al., 2015). We therefore examined the function of miR-16 in cell proliferation and apoptosis in SCC-25 and CAL-27 cell lines by the miR-16 mimic and inhibitor. Results indicated that miR-16 overexpression led to inhibition of cell proliferation and induction of apoptosis, whereas miR-16 knockdown induced promotion of cell proliferation and suppression of apoptosis. These data indicate that miR-16 plays a tumor-suppressive role in OSCC.

We further searched the potential target gene of miR-16 using a bioinformatics tool and found that AKT3 and BCL2L2 are downstream target mRNAs. AKT3 is a homologous gene that belongs to the serine/threonine protein kinase AKT subfamily. Once AKT3 has been hyperactivated in tumorigenesis, it could be a vulnerable node to be targeted (Zboray, Mohrherr, Stiedl, Pranz, & Wandruszka, 2017). The expression and activation of AKT3 mediates cancer progression and controls cellular processes such as cell growth, proliferation, apoptosis, and invasion (Kim et al., 2016). As an oncogene, AKT3 was found to be upregulated in many types of cancers by enhancing the activity of cancer cells (Madhunapantula & Robertson, 2017; Mure et al., 2010; Shao & Aplin, 2010), whereas knockdown of AKT3 isoforms has been reported to abrogate the growth of tumors through inducing cell apoptosis and inhibiting proliferation (Paul-Samojedny et al., 2014, 2015). Moreover, emerging evidence suggests that AKT3 was regulated by a series of miRNAs, such as miR-29b (Li et al., 2017), miR-582 (Jin et al., 2017), miR-497 (Zhuang et al., 2017), and miR-338 (Sui et al., 2017), which could suppress cancer progression. In line with these findings, AKT3 was also identified as a target gene of miR-16 in this study. Luciferase activity
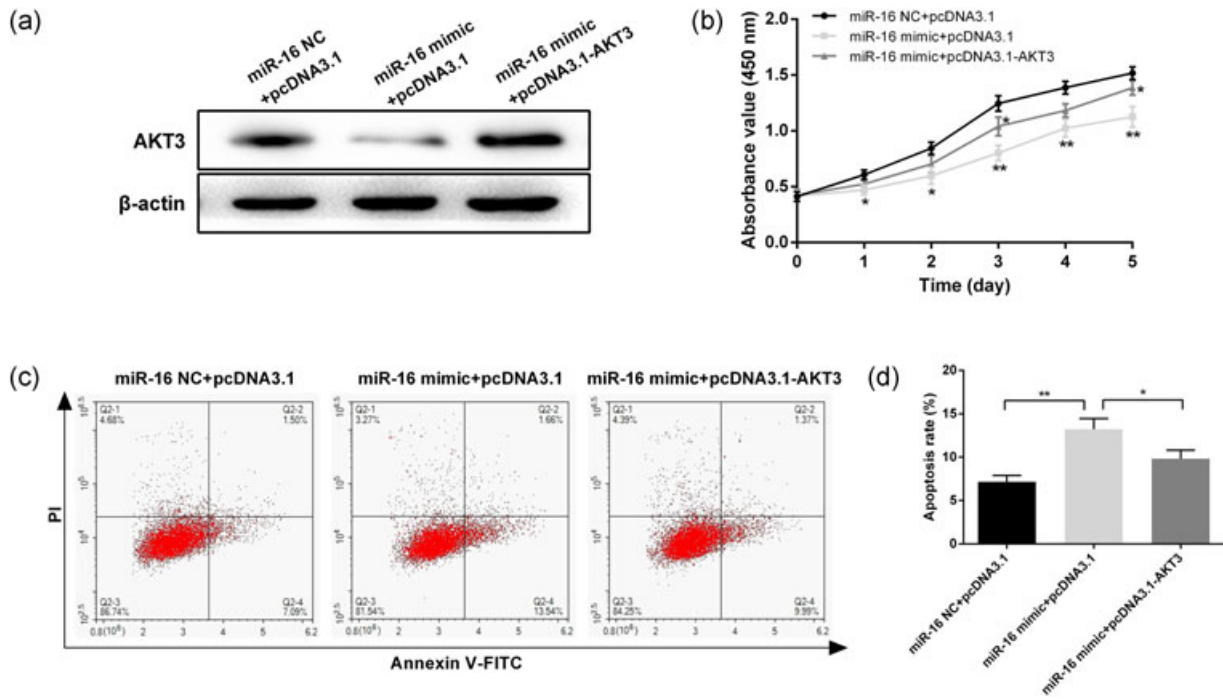
FIGURE 6 Overexpression of AKT3 promotes proliferation and inhibits apoptosis in SCC-25 cells. (a) Protein expression of AKT3 was measured by western blot in SCC-25 cells after cotransfection with pcDNA3.1-AKT3 and miR-16. (b) Cell proliferation was measured at 24, 48, 72, 96, and 120 hr after transfection by CCK-8. (c) Annexin V/PI staining analysis was performed to investigate the apoptosis of SCC-25 cells. (d) The histogram showed the apoptosis rate of SCC-25 cells. Data were presented as mean ± standard deviation for three independent experiments. *$p < 0.05$, **$p < 0.01$, ***$p < 0.001$ versus the negative control [Color figure can be viewed at wileyonlinelibrary.com]
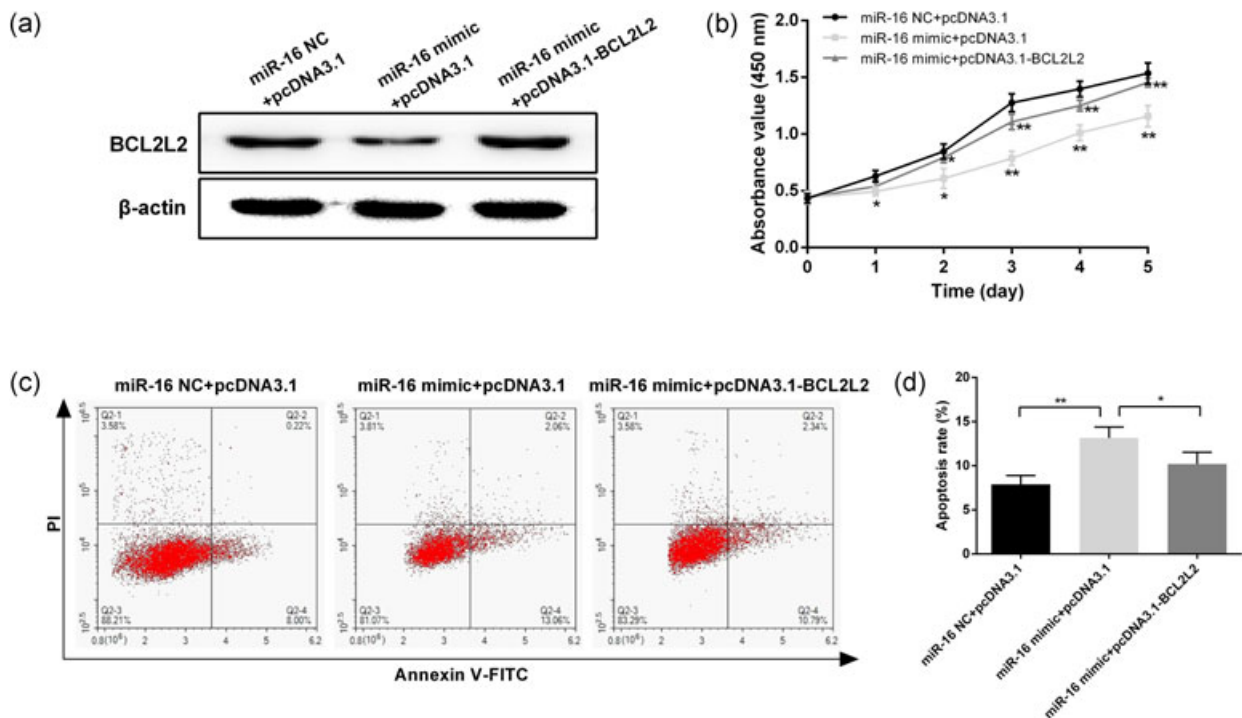

FIGURE 7 Overexpression of BCL2L2 promotes proliferation and inhibits apoptosis in SCC-25 cells. (a) Protein expression of BCL2L2 was measured by western blot in SCC-25 cells after cotransfection with pcDNA3.1- BCL2L2 and miR-16. (b) Cell proliferation was measured at 24, 48, 72, 96, and 120 hr after transfection by CCK-8. (c) Annexin V/PI staining analysis was performed to investigate the apoptosis of SCC-25 cells. (d) The histogram showed the apoptosis rate of SCC-25 cells. Data were presented as mean ± standard deviation for three independent experiments. *$p < 0.05$, **$p < 0.01$, ***$p < 0.001$ versus the negative control. miR-16, microRNA-16 [Color figure can be viewed at wileyonlinelibrary.com]
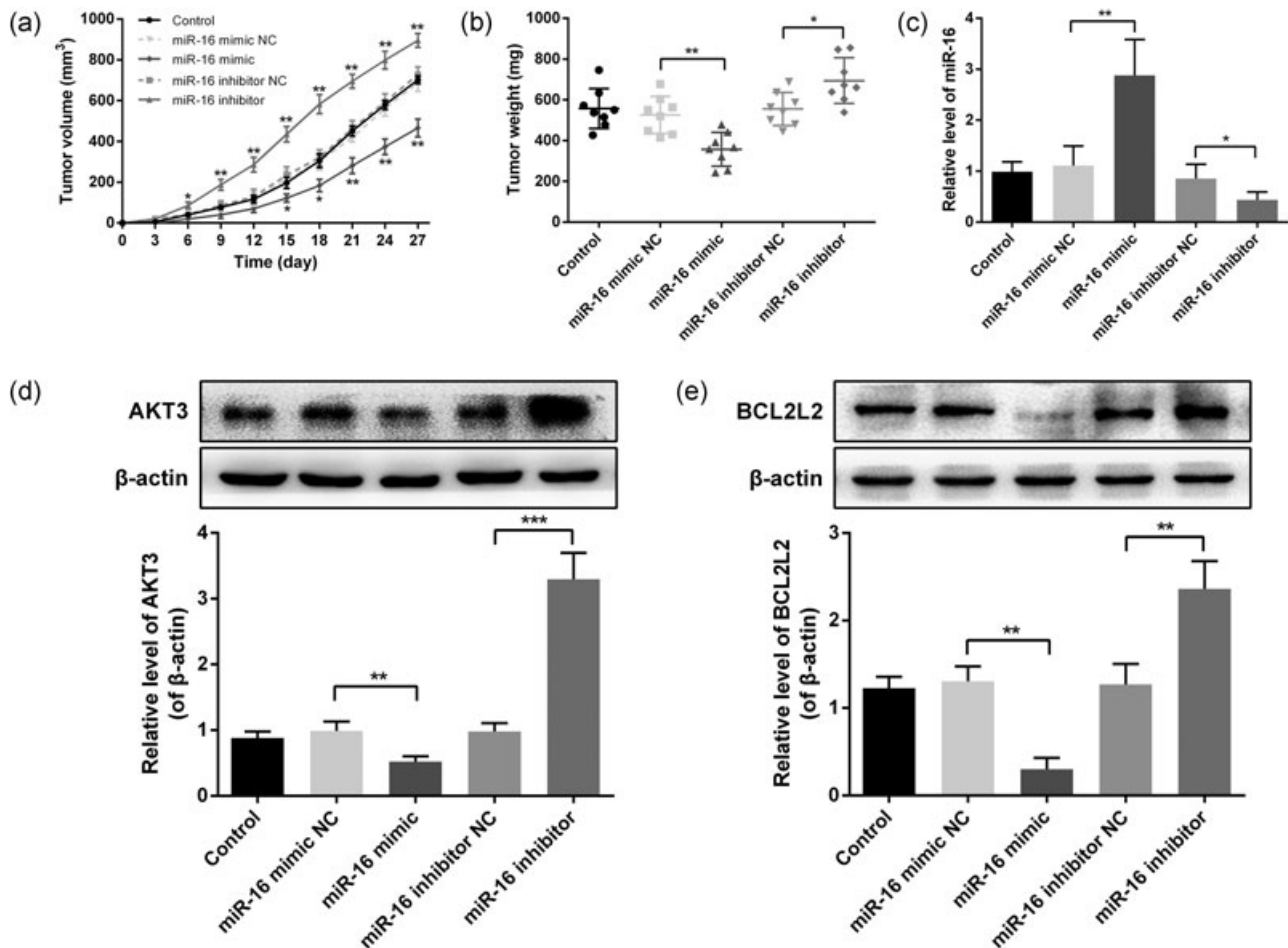
FIGURE 8 miR-16 inhibits SSC-25 engrafted tumor growth in vivo. SCC-25 cells transfected with the miR-16 mimic/inhibitor or scramble were injected into nude mice to generate a xenograft model. (a) Tumor size was measured every three days and calculated as length × width^2/2. (b) Xenograft tumors were weighed on the 27th day after inoculating. (c) The relative miR-16 expression in xenografts was analyzed by qRT-PCR. (d) Protein expression of AKT3 in xenografts was measured by western blot. (e) Protein expression of BCL2L2 in xenografts was measured by western blot. Data were presented as mean ± standard deviation. *$p < 0.05$, **$p < 0.01$, ***$p < 0.001$ versus the negative control. miR-16, microRNA-16; qRT-PCR, quantitative reverse transcription polymerase chain reaction
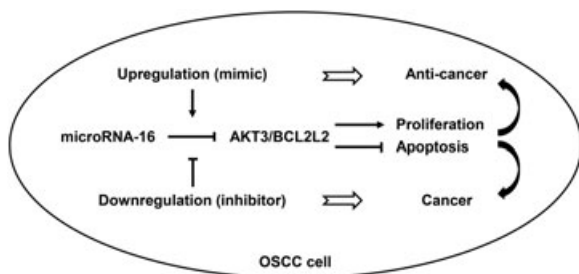

FIGURE 9 Schematic illustration of the proposed mechanisms of miR-16 functions as a tumor suppressor in oral squamous cell carcinoma (OSCC). MiR-16 is downregulated in OSCC tissues and cell lines. It could inhibit cell proliferation and induce apoptosis by directly targeting AKT3 and BCL2L2. Downregulation of miR-16 exerts a carcinogenic effect, whereas upregulation of miR-16 plays an anticancer role in OSCC. miR-16, microRNA-16

assay indicated that AKT3 was the direct downstream target of miR-16 in OSCC. The correlation analysis and qRT-PCR revealed a negative relationship between miR-16 and AKT3 in OSCC patients and cell lines. More important, AKT3 was found to mediate the functional influence of miR-16 on cell proliferation and apoptosis in vitro and in vivo experiments.

BCL2L2, a prosurvival member of the BCL2 protein family, has been reported to function as an oncogene in reducing apoptosis and promoting cell survival (Qu et al., 2015). The activation of BCL2L2 is closely related to the occurrence and progression of tumors. It was reported that BCL2L2 was upregulated in diverse human malignancies (Lu et al., 2016; Wang, Liu, Li, & Tang, 2013). We proved that miR-16 downregulated the mRNA and protein expressions of BCL2L2 through directly binding the 3′-UTR site. The inverse correlation between miR-16 and BCL2L2 levels in OSCC tissues supported this conclusion. In addition, we verified that overexpression of BCL2L2 counteracted the effects of miR-16 on cell

proliferation and apoptosis as well as tumor growth in xenograft mice. Together, our data provide evidence that miR-16 may inhibit proliferation and induce apoptotic signals at least in part through reducing the expression of AKT3 and BCL2L2.

In addition to AKT3 and BCL2L2, some other genes were also identified as the potential downstream targets of miR-16, such as YAP1 and Cyclin E1. These genes were reported to be related to diverse cancers. For example, a previous study indicated that YAP1 saved an oncogenic function in gastric adenocarcinoma development, and elevated cyclin E1 is associated with breast cancer and present throughout the cancer cell cycle (Guo et al., 2015; Kang et al., 2015). The functions and mechanisms of these genes regulated by miR-16 in OSCC still need to be explored in further studies. Besides, the limitation in this study is that the sample size was small; there were only eighteen OSCC patients. Although this does not affect the results, the expression of miR-16 would be further verified in a larger cohort of OSCC patients.

In summary, this study revealed that miR-16 was downregulated in OSCC tissues and cell lines, and it inhibited cell proliferation and induced apoptosis through decreasing the downstream genes AKT3 and BCL2L2. To our knowledge, this report is the first to suggest that miR-16 acts as a tumor-suppressor miRNA in OSCC by directly targeting AKT3 and BCL2L2. The findings will improve our understanding of the mechanisms involved in cancer progression and provide novel targets for the molecular treatment of OSCC.

CONFLICTS OF INTEREST

The authors declare no conflicts of interest.

ORCID

Guang-hui Li http://orcid.org/0000-0003-3928-5878

REFERENCES

Chi, A. C., Day, T. A., & Neville, B. W. (2015). Oral cavity and oropharyngeal squamous cell carcinoma – An update. *CA: A Cancer Journal for Clinicians, 65*, 401–421.

Feng, X., Luo, Q., Wang, H., Zhang, H., & Chen, F. (2018). MicroRNA-22 suppresses cell proliferation, migration and invasion in oral squamous cell carcinoma by targeting NLRP3. *Journal of Cellular Physiology*. Advance online publication. https://doi.org/10.1002/jcp.26331

Fukumoto, I., Hanazawa, T., Kinoshita, T., Kikkawa, N., Koshizuka, K., Goto, Y., ... Seki, N. (2015). MicroRNA expression signature of oral squamous cell carcinoma: Functional role of microRNA-26a/b in the modulation of novel cancer pathways. *British Journal of Cancer, 112*, 891–900.

Guo, X., Connick, M., Vanderhoof, J., Ishak, M. A., & Hartley, R. (2015). MicroRNA-16 modulates HuR regulation of cyclin E1 in breast cancer cells. *International Journal of Molecular Sciences, 16*, 7112–7132.

Hunt, S., Jones, A. V., Hinsley, E. E., Whawell, S. A., & Lambert, D. W. (2011). MicroRNA-124 suppresses oral squamous cell carcinoma motility by targeting ITGB1. *FEBS Letters, 585*, 187–192.

Jiang, Q. Q., Liu, B., & Yuan, T. (2013). MicroRNA-16 inhibits bladder cancer proliferation by targeting Cyclin D1. *Asian Pacific Journal of Cancer Prevention, 14*, 4127–4130.

Jin, Y., Tao, L. P., Yao, S. C., Huang, Q. K., Chen, Z. F., Sun, Y. J., & Jin, S. Q. (2017). MicroRNA-582-5p suppressed gastric cancer cell proliferation via targeting AKT3. *European Review for Medical and Pharmacological Sciences, 21*, 5112–5120.

Kang, W., Tong, J. H., Lung, R. W., Dong, Y., Zhao, J., Liang, Q., ... To, K. F. (2015). Targeting of YAP1 by microRNA-15a and microRNA-16-1 exerts tumor suppressor function in gastric adenocarcinoma. *Molecular Cancer, 14*, 52.

Kim, M., Kim, Y. Y., Jee, H. J., Bae, S. S., Jeong, N. Y., Um, J. H., & Yun, J. (2016). Akt3 knockdown induces mitochondrial dysfunction in human cancer cells. *Acta Biochimica et Biophysica Sinica, 48*, 447–453.

Lai, Y. H., Liu, H., Chiang, W. F., Chen, T. W., Chu, L. J., Yu, J. S., ... Tan, B. C. M. (2018). MiR-31-5p-ACOX1 axis enhances tumorigenic fitness in oral squamous cell carcinoma via the promigratory prostaglandin E2. *Theranostics, 8*, 486–504.

Li, Y., Cai, B., Shen, L., Dong, Y., Lu, Q., Sun, S., ... Chen, J. (2017). MiRNA-29b suppresses tumor growth through simultaneously inhibiting angiogenesis and tumorigenesis by targeting Akt3. *Cancer Letters, 397*, 111–119.

Lin, S., & Gregory, R. I. (2015). MicroRNA biogenesis pathways in cancer. *Nature Reviews Cancer, 15*, 321–333.

Lu, W., Feng, L., Zhang, Y., Ma, Y., Li, P., Wang, Y., ... Lou, W. (2016). MiR-15a induces cell apoptosis by targeting BCL2L2 and BCL2 in HPV-positive hypopharyngeal squamous cell carcinoma. *Oncology Reports, 36*, 2169–2176.

Ma, Q., Wang, X., Li, Z., Li, B., Ma, F., Peng, L., ... Jiang, B. (2013). MicroRNA-16 represses colorectal cancer cell growth in vitro by regulating the p53/survivin signaling pathway. *Oncology Reports, 29*, 1652–1658.

Madhunapantula, S. V., & Robertson, G. P. (2017). Targeting protein kinase-b3 (akt3) signaling in melanoma. *Expert Opinion on Therapeutic Targets, 21*, 273–290.

Manikandan, M., Deva Magendhra Rao, A. K., Arunkumar, G., Manickavasagam, M., Rajkumar, K. S., Rajaraman, R., & Munirajan, A. K. (2016). Oral squamous cell carcinoma: MicroRNA expression profiling and integrative analyses for elucidation of tumourigenesis mechanism. *Molecular Cancer, 15*, 28.

Mobarra, N., Shafiee, A., Rad, S. M., Tasharrofi, N., Soufi-zomorod, M., Hafizi, M., ... Soleimani, M. (2015). Overexpression of microRNA-16 declines cellular growth, proliferation and induces apoptosis in human breast cancer cells. *In Vitro Cellular & Developmental Biology – Animal, 51*, 604–611.

Mure, H., Matsuzaki, K., Kitazato, K. T., Mizobuchi, Y., Kuwayama, K., Kageji, T., & Nagahiro, S. (2010). Akt2 and Akt3 play a pivotal role in malignant gliomas. *Neuro-oncology, 12*, 221–232.

Omar, E. (2015). Current concepts and future of noninvasive procedures for diagnosing oral squamous cell carcinoma – A systematic review. *Head & Face Medicine, 11*, 6.

Osada, H., & Takahashi, T. (2007). MicroRNAs in biological processes and carcinogenesis. *Carcinogenesis, 28*, 2–12.

Paul-Samojedny, M., Pudełko, A., Kowalczyk, M., Fila-Daniłow, A., Suchanek-Raif, R., Borkowska, P., & Kowalski, J. (2015). Knockdown of AKT3 and PI3KCA by RNA interference changes the expression of the genes that are related to apoptosis and autophagy in T98G glioblastoma multiforme cells. *Pharmacological Reports, 67*, 1115–1123.

Paul-Samojedny, M., Suchanek, R., Borkowska, P., Pudełko, A., Owczarek, A., Kowalczyk, M., ... Kowalski, J. (2014). Knockdown of AKT3 (PKBγ) and PI3KCA suppresses cell viability and proliferation and induces the

apoptosis of glioblastoma multiforme T98G cells. *BioMed Research International*, 2014, 1–12.

Qu, J., Zhao, L., Zhang, P., Wang, J., Xu, N., Mi, W., … Qu, J. (2015). MicroRNA-195 chemosensitizes colon cancer cells to the chemotherapeutic drug doxorubicin by targeting the first binding site of BCL2L2 mRNA. *Journal of Cellular Physiology*, 230, 535–545.

Radhika, T., Jeddy, N., Nithya, S., & Muthumeenakshi, R. M. (2016). Salivary biomarkers in oral squamous cell carcinoma – An insight. *Journal of Oral Biology and Craniofacial Research*, 6, S51–S54.

Rivera, C., Oliveira, A. K., Costa, R. A. P., de Rossi, T., & Paes Leme, A. F. (2017). Prognostic biomarkers in oral squamous cell carcinoma: A systematic review. *Oral Oncology*, 72, 38–47.

Shao, Y., & Aplin, A. E. (2010). Akt3-mediated resistance to apoptosis in B-RAF-targeted melanoma cells. *Cancer Research*, 70, 6670–6681.

Sui, G., Fei, D., Guo, F., Zhen, X., Luo, Q., Yin, S., & Wang, H. (2017). Original article microRNA-338-3p inhibits thyroid cancer progression through targeting AKT3. *American Journal of Cancer Research*, 7, 1177–1187.

Tu, H. F., Lin, S. C., & Chang, K. W. (2013). MicroRNA aberrances in head and neck cancer. *Current Opinion in Otolaryngology & Head and Neck Surgery*, 21, 104–111.

Wang, F., Liu, M., Li, X., & Tang, H. (2013). MiR-214 reduces cell survival and enhances cisplatin-induced cytotoxicity via down-regulation of Bcl2l2 in cervical cancer cells. *FEBS Letters*, 587, 488–495.

Wang, Y. J., Zhang, Z. F., Fan, S. H., Zhuang, J., Shan, Q., Han, X. R., … Zheng, Y. L. (2017). MicroRNA-433 inhibits oral squamous cell carcinoma cells by targeting FAK. *Oncotarget*, 8, 100227–100241.

Wu, W. L., Wang, W. Y., Yao, W. Q., & Li, G. D. (2015). Suppressive effects of microRNA-16 on the proliferation, invasion and metastasis of hepatocellular carcinoma cells. *International Journal of Molecular Medicine*, 36, 1713–1719.

Zboray, K., Mohrherr, J., Stiedl, P., Pranz, K., & Wandruszka, L. (2017). AKT3 drives adenoid cystic carcinoma development in salivary glands. *Cancer Medicine*.

Zhang, B., Li, Y., Hou, D., Shi, Q., Yang, S., & Li, Q. (2017). MicroRNA-375 inhibits growth and enhances radiosensitivity in oral squamous cell carcinoma by targeting insulin like growth factor 1 receptor. *Cellular Physiology and Biochemistry*, 42, 2105–2117.

Zhuang, J., Ye, Y., Wang, G., Ni, J., He, S., Hu, C., … Lv, Z. (2017). MicroRNA-497 inhibits cellular proliferation, migration and invasion of papillary thyroid cancer by directly targeting AKT3. *Molecular Medicine Reports*, 16, 5815–5822.